Conformational Changes in Pediocin AcH upon Vesicle Binding and Approximation of the Membrane-Bound Structure in Detergent Micelles†

Rachel M. Watson,‡ Robert W. Woody,§ Randolph V. Lewis,‡ D. Scott Bohle,|| Amy H. Andreotti,⊥ Bibek Ray,# and Kurt W. Miller*,‡

Departments of Molecular Biology, Animal Science, and Chemistry, University of Wyoming, Laramie, Wyoming 82071, Department of Biochemistry and Molecular Biology, Colorado State University, Fort Collins, Colorado 80523, and Department of Biochemistry, Biophysics, and Molecular Biology, Iowa State University, Ames, Iowa 50011

Received May 21, 2001; Revised Manuscript Received September 18, 2001

ABSTRACT: Pediocin AcH is a 44-residue antimicrobial peptide with bactericidal potency against Gram-positive bacteria such as *Listeria*. It belongs to a family of bacteriocins that, when membrane-associated, is predicted to contain β-sheet and α-helical regions. All bacteriocins in this family have a conserved N-terminal disulfide bond. An additional C-terminal disulfide bond in pediocin AcH is thought to confer enhanced potency and broader specificity range against sensitive bacteria. The C-terminal disulfide bond may also affect the conformation of the C-terminus. The secondary structures of pediocin AcH in aqueous solution and vesicles from susceptible cells, as well as the ability of trifluoroethanol (TFE) and detergent systems to induce secondary structures like those induced in vesicles, were studied by circular dichroism (CD) spectroscopy. Like related peptides, pediocin AcH was highly unordered in aqueous solution, 56%. However, it also contained 20% β-strand and 15% β-turn structures. Upon complete binding to vesicles, 32% α-helical structure formed, the unordered structure decreased to 32%, and the β-strand and β-turn structures remained largely unchanged. Thus, a $\beta\alpha$ domain structure formed in vesicles. The helical structure likely forces the C-terminal tail to loop back on the helix so that the C24−C44 disulfide bond can form. Detergent micelles were superior to TFE in their ability to induce secondary structural fractions in pediocin AcH comparable to those observed in vesicles. This demonstrates the importance of a hydrocarbon−water interface to pediocin AcH structure induction and suggests that it is preferable to use detergent micelles as solvents in NMR studies of pediocin AcH structure.

Antimicrobial peptides are lethal weapons used by all organisms to ward off competitors or provide a first-line defense against infection (*1*−*3*). Peptides known as bacteriocins produced by the lactic acid bacteria are one source of these bactericides (*4*). The class IIa group studied here is heat-stable, 37−48 amino acids in length, and has potent antilisterial activity (*5*). These peptides exert bactericidal activity by forming pores in target cell membranes (*6*). Class IIa peptides contain at least one conserved disulfide bond, a highly conserved N-terminal YGNGV sequence, and a moderately conserved hydrophobic C-terminal domain (*5*, *7*).

Pediocin AcH (also known as pediocin PA-1) is a 44 amino acid class IIa bacteriocin produced by some strains in the genus *Pediococcus*. Its sequence is highly homologous to other class IIa bacteriocins (Table 1) (*8*−*18*). Pediocin AcH, coagulin, divercin V41, and enterocin A are unusual in that they contain two disulfide bonds (*8*, *9*, *11*). Despite the homology between class IIa bacteriocins, target cell specificities and potencies vary (*19*−*21*). For example, pediocin AcH and enterocin A have enhanced potency and activity spectra compared to sakacin P and curvacin A. This enhancement may be conferred by the second disulfide bond that, when reduced or removed, decreases potency drastically (*19*, *22*, *23*) and, when introduced into sakacin P, broadens target cell specificity and increases activity at higher temperatures (*24*).

The two- and three-dimensional structures of pediocin AcH, before and after membrane binding, are unknown. Analysis of other bacteriocins suggests that conformations are largely unordered before binding and become structured only after membrane binding (*21*, *25*−*27*). Chen et al. predict three β-strands in the first 17 amino acids of pediocin PA-1 (*28*). They further suggest that the GNGV portion of the YGNGV sequence forms the first β-turn of the β-sheet and that strands 2 and 3 are linked by the C9−C14 disulfide bond. These predictions are supported by NMR[1] analysis of leucocin A in 90% TFE and DPC micelles. This peptide contains a three-strand antiparallel β-sheet within residues 2−16 that is cross-linked by the disulfide (*27*).

† This work was supported by the State of Wyoming, the NSF EPSCOR program, and NIH Grant GM 22994.

* Corresponding author. Phone: 307-766-2037. Fax: 307-766-5098. E-mail: kwmiller@uwyo.edu.

‡ Department of Molecular Biology, University of Wyoming.

§ Colorado State University.

|| Department of Chemistry, University of Wyoming.

⊥ Iowa State University.

Department of Animal Science, University of Wyoming.

[1] Abbreviations: CD, circular dichroism spectroscopy; CMC, critical micelle concentration; DPC, dodecylphosphocholine; HPLC, high-performance liquid chromatography; NMR, nuclear magnetic resonance; PL, phospholipid; RMS, root mean square; SDS, sodium dodecyl sulfate; SVD, singular value decomposition; TFE, trifluoroethanol.

10.1021/bi011031p CCC: $20.00
Published on Web 10/26/2001

Table 1: Sequences of Some YGNGV Bacteriocins

Pediocin AcH	KYYGNGVTCGKHSCSVDWGKATTCIINNGAMAWATGGHQGNHKC	(11,15,16)
Coagulin	KYYGNGVTCGKHSCSVDWGKATTCIINNGAMAWATGGHQGTHKC	(14)
Divercin V41	TKYYGNGVYCNSKKCWVDWGQASGCIGQTVVGGWLGGAIPGKC	(9)
Enterocin A	TTHSGKYYGNGVYCTKNKCTVDWAKATTCIAGMSIGGFLGGAIPGKC	(8)
Leucocin A	KYYGNGVHCTKSGCSVNWGEAFSAGVHRLANGGNGFW	(10)
Mesentericin Y105	KYYGNGVHCTKSGCSVNWGEAASAGIHRLANGGNGFW	(10)
Carnobacteriocin B2	VNYGNGVSCSKTKCSVNWGQAFQERYTAGINSFVSGVASGAGSIGRRP	(17)
Sakacin A/curvacin A	ARSYGNGVYCNNKKCWVNRGEATQSIIGGMISGWASGLAGM	(12,17)
Sakacin 674/sakacin P	KYYGNGVHCGKHSCTVDWGTAIGNIGNNAAANWATGGNAGWNK	(18,13)

On the basis of Chou and Fasman sequence analysis, the C-terminal nonpolar regions of class IIa peptides are predicted to form α-helices (*25*). These helices are amphipathic (*20*) and could promote interaction with and perturbation of cell membranes. NMR studies of leucocin A in 90% TFE and DPC micelles, and carnobacteriocin B2 in 90% TFE, confirm that α-helices form in this region. In leucocin A, the helix corresponds to residues 17−31 in the C-terminal domain, and in carnobacteriocin B2, a helical structure extends from residues 18 to 39 (*1*, *27*).

Although evidence supports a $\beta\alpha$ structure for membrane-bound class IIa bacteriocins, the structure of a peptide with two disulfides has not been determined. It is possible that the second disulfide could enhance peptide stability in aqueous solution and alter the structure of the C-terminus. To examine these possibilities, secondary structures of pediocin AcH were determined in water and in vesicles made from phospholipids extracted from susceptible cells. Structure also was studied in TFE and detergents to find systems that induce structures comparable to those formed in vesicles and to illuminate environmental features needed for structure induction. The technique selected for these studies was circular dichroism spectroscopy (CD) as it is amenable for study of peptides in both vesicles and other solvents (*29*−*31*). Structural predictions obtained by CD often agree well with NMR and X-ray determinations (*32*). The results show that, unlike related bacteriocins, pediocin AcH contains some β-structure in aqueous solution. Upon membrane binding, a $\beta\alpha$ domain structure forms. A hydrocarbon−water interface is important to structure induction, as detergent micelles were superior to TFE in inducing secondary structure fractions comparable to those observed in vesicles.

EXPERIMENTAL PROCEDURES

Production, Isolation, and Purification of Pediocin AcH. Pediocin AcH was isolated from a 60 L combined culture volume of *Pediococcus acidilactici* strain LB42-923 (*33*). Cultures were grown without shaking for 18 h at 37 °C in 2× tryptone, glucose, and yeast extract (TGE) broth containing 0.2% Tween-80 detergent (*34*). The OD at 600 nm was between 1 and 2, and the terminal pH of the culture broth was between 3.6 and 3.8 at the time of harvest. Crude pediocin AcH was obtained from this strain by the previously published cell adsorption−desorption method (*34*). This process included heat-treating the culture to stop culture growth, kill cells, and denature proteases, followed by adjustment of the culture pH to 6.5 with 10 M NaOH. The pH change permitted the peptide to adsorb to the cells. Cells were then harvested, washed, and resuspended to 1/10th volume in 0.1 M lactic acid and 0.1 M NaCl (final pH of 1.5−2.0) that, after an overnight stir, caused the peptide to desorb from the cell surface. The supernatant, containing the peptide, was then dialyzed against distilled water, freeze-dried, and stored at −20 °C. Further purification of pediocin AcH was accomplished using HPLC. The crude, dry powder from a 1 L preparation was dissolved in 2 mL of distilled water. It was brought into solution at 37 °C and then centrifuged to remove particulates. Any remaining particulates were removed by filtration through a 0.45 μm filter. Finally, the peptide was acidified with TFA to 0.1%. The solution was loaded onto a 1.0 × 25 cm, 100 μm pore diameter C18 semipreparative reverse-phase HPLC column (Vydac) connected to a Hitachi HPLC apparatus. Peptide was eluted at 4.9 mL/min over the course of 1 h using a linear 0−50% 2-propanol−water−0.1% TFA gradient. The fraction containing activity was hand-collected, freeze-dried, taken up in 1 mL of 0.1% TFA−water, rechromatographed, and collected under the same conditions. Peptide recoveries were determined by reading the A_{280nm} values of fractions using bovine serum albumin as a calibration standard. Actual concentrations of pediocin AcH in HPLC fractions were obtained by applying a correction factor, determined by amino acid analysis, to the A_{280nm} readings.

Characterization of Pediocin AcH by Mass Spectrometry. Pediocin AcH was analyzed by electrospray mass spectrometry using a Finnigan LCQ ion-trap mass spectrometer. A deconvoluted mass spectrum was obtained by direct injection of 100 μL of a 50 μM solution of pediocin AcH in 0.025% TFA.

Phospholipid Extraction and Preparation of Phospholipid Vesicles. Phospholipids were extracted from *Listeria innocua* Lin11 using the Bligh and Dyer two-phase extraction with some modifications by Kates and Winkowski (*35*−*37*). A 2 L culture was grown to an OD at 600 nm of 0.6. Cells were harvested and washed in 0.1% peptone water. The final pellet was weighed and resuspended in 1 mL of 0.1 M HCl for

every 400 mg of wet cell weight. The resuspension was split into 1 mL aliquots, and methanol and chloroform were added to bring the final mixture ratio to 2:1:1 methanol:chloroform: 0.1 M HCl. The mixture was then vortexed intermittently in the presence of glass beads (0.10−0.15 mm in diameter) over a 1 h period (*37*). After centrifugation, the supernatant was set aside, and the pellet was rinsed again with 2:1:1 methanol: chloroform:0.1 M HCl. The supernatants were pooled, and HCl and chloroform were added to achieve a 1:1:1 methanol: chloroform:0.1 M HCl ratio. The lower chloroform phase was collected and neutralized with 0.5 M ammonium hydroxide in methanol. Phospholipids were dried down, resuspended in 9:1 chloroform:methanol, and stored under nitrogen at −20 °C for 2 weeks or less. Concentrations of the phospholipids were determined using the Bartlett phosphorus assay (*36*). Large unilamellar vesicles (LUVs) were created using the extrusion method described by Lipex Biomembranes Inc. (Vancouver, Canada). Phospholipids derived from *L. innocua* Lin11 were dried down at 30 °C under a stream of nitrogen. Trace solvent was removed by placing the phospholipid film in an evacuation chamber for 1 h. The lipid film was then resuspended in 10 mM 2-(*N*-morpholino)ethanesulfonic acid potassium salt (KMES) buffer (pH 6.0) by extensive vortexing and intermittent warming to 50 °C. Five freeze−thaw cycles were then performed on the resuspension. These freeze−thaw cycles consisted of 1.5 min in dry ice/ethanol followed by 1.5 min in 50 °C water. The mixture was vortexed extensively between freeze−thaw cycles. LUVs were then created by 10 successive passes through a Lipex Biomembranes thermobarrel extruder at 30 °C. Two 50 nm filters were used, and vesicles of 70−80 nm in diameter typically are produced under these conditions (Lipex Biomembranes). The final concentration of the vesicles was determined using the Bartlett phosphorus assay (*36*).

Circular Dichroism Spectroscopy. For the first set of CD experiments, purified pediocin AcH was added to *L. innocua*-derived phospholipid vesicles, buffered to a pH of 6 with KMES buffer, in the following peptide to phospholipid ratios: 1:35, 1:50, 1:70, 1:140, 1:185, and 1:215. To attain these ratios, the peptide concentration was fixed at 20 μM, over a range of phospholipid concentrations: 0.7, 1.0, 1.4, 2.8, 3.7, and 4.3 mM. Lower ratios of peptide to phospholipid were achieved by varying the peptide concentration at a fixed phospholipid concentration of 7.2 mM. The following peptide to phospholipid molar ratios were obtained in this manner: 1:225, 1:562, and 1:1125. Peptide concentrations were 32.0, 12.8, and 6.4 μM, respectively. Data were also collected for 20 μM peptide in 1 mM KMES buffer; 10%, 20%, 50%, and 90% trifluoroethanol (TFE); 1, 5, 10, and 30 mM sodium dodecyl sulfate (SDS); 0.5, 2, 5, and 10 mM DPC; and mixed micelles composed of 7 mM SDS and 3 mM DPC. All TFE and detergent solutions were buffered to a pH of 6 with 1 mM KMES. For SDS the critical micellar concentration of 4.5 mM at 22 °C was determined by the method of Vulliez-Le Normand et al. (*38*). The CD spectrophotometer used for data collection was a Jasco J-720. CD spectra were recorded between 184 and 260 nm for samples in TFE and between 190 and 260 nm for all others. A thermally controlled (22 °C) quartz cell with a 0.2 mm path length was used. Data were collected every 0.1 nm and, with one exception, were the average of 20 scans. In the case of the 6.4 μM peptide sample, 80 scans were averaged rather than 20 to improve the signal to noise ratio. The bandwidth was set at 1.0 nm and the sensitivity at 10 mdeg, and the response time was 4 s. In all cases baseline scans of aqueous buffer, vesicles, or detergent alone were subtracted from the experimental readings. Results are expressed in units of molar CD per residue [$\Delta\epsilon/n$ (cm^2/mmol)] and plotted versus wavelength.

When CD spectra for peptides or proteins in membrane suspensions are collected, the potentially distorting effects of light scattering as well as the possible manifestations of absorption flattening must be considered (*39*). These effects were minimized by using a short path length cell and positioning the sample cell close to the photomultiplier tube to maximize the collection of scattered light. Baseline contributions from vesicles containing no peptide were subtracted from all sample scans containing peptide. Light scattering for pediocin AcH in vesicles and the other solvents was monitored both by visual observation and spectrophotometrically by turbidity at 400 nm. Light scattering due to aggregation was only observed for high ratios of peptide to anionic lipid. At low molar ratios, $<1/140$, the light scattering approached zero and was comparable to scattering of peptide in aqueous solution. All quantitative comparisons of structures formed in solvents and vesicles were made in this region.

CD Data Analysis. Analysis of the CD spectra was performed both qualitatively and quantitatively. For qualitative analysis, $\Delta\epsilon/n$ values were recorded every 0.1 nm, corrected for baseline readings, and displayed every 1 nm using Math Soft Axum 6.0 software. A spline function was fit to the data and setting the degrees of freedom to 20 controlled the smoothness of the spline fit. Spectral features, such as the wavelengths of positive and negative maxima in $\Delta\epsilon/n$, which are characteristic of certain types of secondary structure, were identified.

Quantitative curve fitting included analysis of $\Delta\epsilon/n$ values, corrected for background scattering, using the CDPro software analysis program (*40*). This program uses three methods for estimating protein secondary structure fractions from CD spectra. These methods are implemented in the software packages CONTIN/LL, SELCON3, and CDSSTR. Each of these three methods uses a different algorithm for analyzing a given protein CD spectrum, but they all use a single data-file structure (*40*). CONTIN/LL is a variant of the CONTIN method (*41*), which uses a constrained statistical regularization procedure to fit the CD spectrum of the protein being analyzed as a linear combination of CD spectra of reference set proteins. SELCON3 is the most recent version of SELCON (*42*). This method includes the spectrum of the protein to be analyzed in the basis set of CD spectral data, and an initial, approximate guess is made for the unknown secondary structure. This guess is the structure of the reference protein most closely matching the protein under analysis. The resulting matrix equation is solved using the singular value decomposition (SVD) algorithm (*43*) and variable selection (*44*) in the locally linearized model (*45*), and the initial guess is replaced by the solution. This process is repeated to attain self-consistency. In the CDSSTR method (*46*), eight reference proteins are selected randomly from the reference set, and solutions are obtained in the self-consistent formalism (*42*), using the SVD algorithm (*43*) and five SVD components. The same protein reference set, consisting of

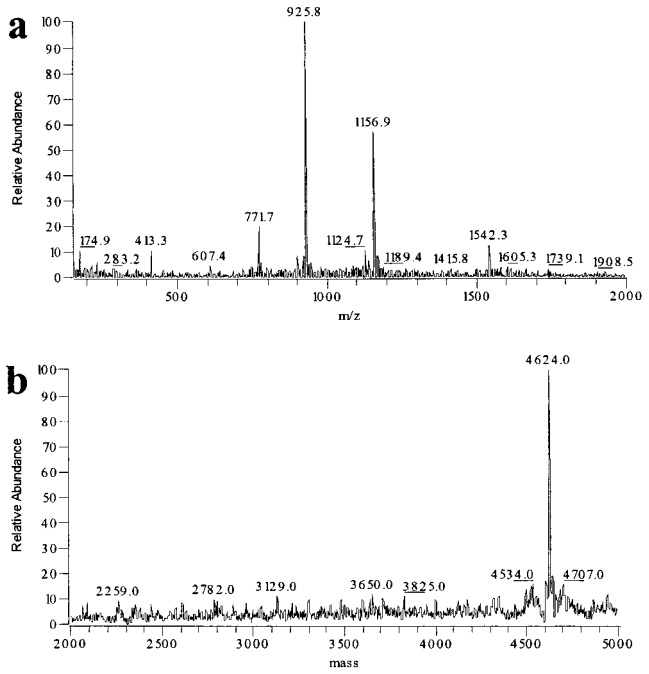

FIGURE 1: (a) Raw and (b) deconvoluted electrospray mass spectra of HPLC-purified pediocin AcH.

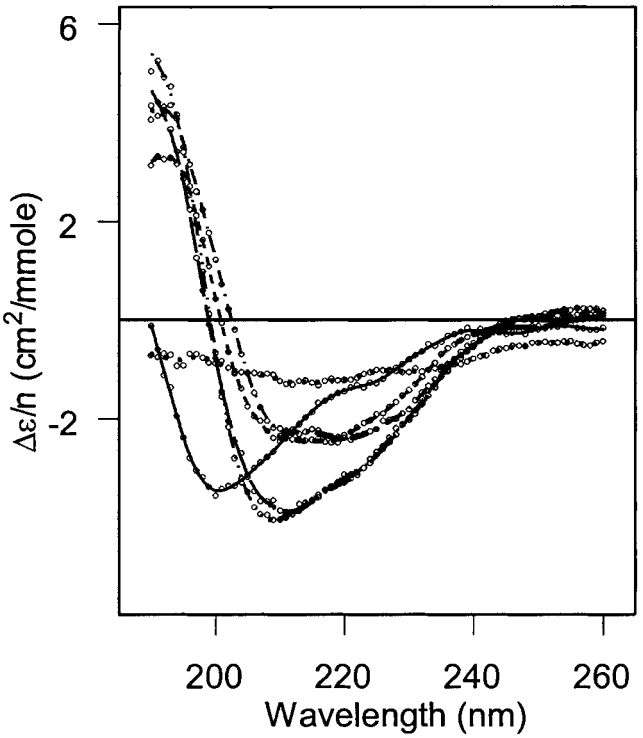

FIGURE 2: CD spectra of pediocin AcH in aqueous solution (—) and vesicles derived from *L. innocua*. Molar ratios of pediocin AcH to phospholipid were 1/35 (•••), 1/50 (—•—), 1/70 (---), 1/140 (— —), and 1/215 (—•••—). $\Delta\epsilon/n$ values are shown every nanometer (○). Curve fitting procedures are described under Experimental Procedures. For simplicity of the figure, peptide to lipid molar ratios of 1/185, 1/562, and 1/1125 were omitted. These curves were, to within experimental error, the same as those for the 1/140 and 1/215 pediocin AcH to phospholipid molar ratios.

43 native and 5 denatured proteins, was used by all methods. This reference set was selected for its fit to the wavelength range of the experimental data. Denatured proteins were included, as they have been found to assist in determining protein secondary structure from CD data for proteins with significant unordered structure (*47*). Output data for each of the three programs were given in terms of fractions of six different secondary structural classes: regular α-helix [H(r)], distorted α-helix [H(d)], regular β-strand [S(r)], distorted β-strand [S(d)], turns (Trn), and unordered (Unrd). Since the same set of reference proteins was used by each of the three programs, their fractional secondary structure outputs could be averaged. For convenience of data interpretation, the distorted and regular components of both helical and strand secondary structural elements were added to give overall helical and strand structures.

RESULTS

Purification of Pediocin AcH. Pediocin AcH was purified by a combination of cell adsorption−desorption enrichment and two cycles of reverse-phase HPLC. Peptide activity eluted from the HPLC column at 29.5% 2-propanol in a linear 0−50% 2-propanol gradient. Approximately 0.3 mg of >95% pure pediocin AcH were obtained per liter of *P. acidilactici* LB42-923 culture broth. The final specific activity was about 4×10^4 AU/μg as measured against the indicator organism *L. innocua* Lin11 (*23*). The final yield of activity corresponded to approximately 2% of the original activity present in the culture medium.

The molecular mass and oxidation state of pediocin AcH were evaluated by electrospray mass spectrometry. The single, multiply charged envelope of ions displayed in the original electrospray mass spectrum (Figure 1a) was deconvoluted, resulting in a molecular ion peak at a molecular weight of 4624 ± 1 Da (Figure 1b). This is the theoretical molecular weight for the disulfide form of pediocin AcH. There was no evidence for the reduced form of the peptide or the methionine sulfoxide species. In addition, no free thiol groups were found by titration with Ellman's reagent, 5,5′-dithiobis(2-nitrobenzoic acid), under assay conditions where 5% of the total thiol groups could be detected if present (data not shown).

CD Analysis of Pediocin AcH in Aqueous Buffer and L. innocua Membrane Vesicles. The CD spectrum of pediocin AcH in aqueous KMES buffer (pH 6) (Figure 2) was characterized by a strong negative maximum at 200 nm. This feature indicated a significant amount of unordered structure in the peptide (*32*). This spectrum differed markedly from spectra seen for the peptide in the presence of vesicles derived from the highly susceptible bacterium *L. innocua.* With the exception of the spectrum for the 1/35 peptide to lipid molar ratio, these spectra were characterized by negative maxima between 208 and 219 nm and positive maxima between 190 and 193 nm. These CD bands were attributed to the induction of some helical content in the peptide (*32*). There was a range of vesicle concentrations at lower peptide to lipid molar ratios (1/140 to 1/1125) over which the CD profiles were very similar. On the basis of the superposition of CD profiles and the comparability of $\Delta\epsilon/n$ values, it was concluded that binding of pediocin AcH to vesicles was essentially complete within this range of peptide to lipid ratios.

In contrast to the above samples, solutions with molar ratios of peptide to phospholipid greater than 1/140 displayed

Table 2: Quantitative Comparison of the Secondary Structure Fractions Induced in Pediocin AcH by Various External Environments

	helix	strand	turn	unordered
aqueous buffer	0.08	0.20	0.15	0.56
vesicles[a]	0.32	0.17	0.19	0.32
10% TFE	0.17	0.18	0.23	0.43
20% TFE	0.24	0.23	0.22	0.31
50% TFE	0.42	0.15	0.18	0.25
90% TFE[b]	0.66	0.05	0.11	0.19
1 mM SDS	0.21	0.27	0.20	0.30
5 mM SDS	0.36	0.18	0.18	0.28
10 mM SDS	0.38	0.15	0.18	0.29
30 mM SDS	0.36	0.15	0.18	0.30
0.5 mM DPC	0.05	0.18	0.12	0.63
2 mM DPC	0.29	0.17	0.20	0.35
5 mM DPC	0.38	0.14	0.17	0.31
10 mM DPC	0.41	0.10	0.16	0.34
7 mM SDS−3 mM DPC	0.34	0.20	0.18	0.28

[a] The molar ratio of pediocin AcH to phospholipid for the vesicle sample was 1/215. The standard deviation for each type of secondary structure was calculated for three preparations at this peptide to lipid molar ratio on three different days. The standard deviation for α-helix, β-strand, β-turn, and unordered fractional structures was 0.0043, 0.0019, 0.0055, and 0.0017, respectively. [b] Fractional secondary structures were obtained by averaging output from CDSSTR and CONTINLL only, as SELCON 3 failed to converge to a satisfactory solution.

noticeable solution turbidity and sample precipitation, which led to a corresponding loss in signal. At peptide to lipid ratios greater than 1/50, there was excessive light scattering and a nearly complete loss of signal, as observed for the ratio 1/35. This behavior was not observed for increasing concentrations of peptide alone in aqueous solution (data not shown). This suggested that aggregation of peptide-bound vesicles was responsible and that absorption flattening (*39*) contributed to the effects on CD. Similar results have been observed in other studies performed with cationic peptides (*30*), and it illustrates the ability of these peptides to tie together pairs of vesicles in solution. Because aggregation interferes with CD readings, ratios greater than 1/140 were not used in secondary structure calculations.

The CD spectra were analyzed to estimate the quantitative distribution of secondary structures induced in pediocin AcH by aqueous buffer and vesicles (Table 2). The spectrum for the 1/215 peptide to lipid molar ratio was selected for data analysis, as it was representative of the spectra with similar CD profiles. Secondary structure analysis indicated that the peptide was 56% unordered in aqueous buffer. Upon binding to vesicles, the percentage of unordered structure decreased to 32%, and the helical structure increased from 8% to 32%. In contrast, changes in the β-strand content (20%−17%) and in the percentage β-turn (15%−19%) were insignificant (see below).

There has been some debate as to whether basis spectra derived from soluble globular proteins are appropriate for the quantitative analysis of the secondary structure distribution in membrane proteins (*48*, *49*). There may be some systematic differences in α-helix and β-sheet contributions to the CD of integral membrane proteins as compared to soluble globular protein CD. These can be attributed to the effects of helix and strand length (*48*−*50*) and to possible differences in the conformation of these secondary structural elements in the two types of proteins (*51*). On the other hand, the polypeptide backbone of proteins, which is responsible for the absorption and CD in the far-UV, is shielded from the bulk solvent by the side chains, and therefore, direct solvent effects on CD are not expected to be significant.

While differences in end effects and conformation could make selection of appropriate basis spectra for membrane proteins and peptides difficult, it should be noted that qualitatively similar problems are encountered in the analysis of globular proteins. The lengths of α-helices and β-strands vary more within the class of soluble globular proteins than they do between globular and membrane proteins. The extent of twist among β-sheets and the curvature of α-helices also show wide variability among globular proteins. Aromatic side-chain contributions further complicate the CD spectra of both types of proteins. For this reason, the method selected for CD secondary structural analysis does not use a single basis spectrum for α-helix, one for β-sheet, etc. Instead, flexible basis sets are used that can adapt to the nature of the protein being analyzed. For example, if a protein contains a number of longer helices that contribute differently to the CD spectrum relative to helices of average length, those proteins among the reference set with longer helices will be given greater weight in the analysis. All of this is done automatically by the variable weighting of the CD spectra from the various reference proteins. This introduction of flexibility in the basis sets has led to significant improvements in performance over the earlier methods that used fixed basis sets. Such flexibility should be able to accommodate most of the CD effects that might be encountered in the membrane-bound proteins. Finally, it should be stressed that the point of our analyses in this paper is not to obtain exact values for the secondary structure fractions but to gain information about trends in the secondary structures as the medium is varied.

CD of Pediocin AcH in TFE and Detergent Micelles. Spectra were collected for pediocin AcH in a range of TFE concentrations (Figure 3). In 10% and 20% TFE, the peptide was significantly unordered, but at high TFE percentages (50% and 90%), helical structure was induced as indicated by the appearance of distinct negative bands at 207−209 nm, negative shoulders near 220 nm, and positive bands at 190 nm. Quantitative analysis of secondary structure distribution in TFE verified that while the helical structure was minimal in 10% TFE, this percentage increased with increasing TFE concentration until, in 90% TFE, pediocin AcH was dominated by 66% α-helix (Table 2). In contrast to the striking rise in α-helical content, there was a general decrease in the β-strand and β-turn structures until in 90% TFE the peptide was only 5% β-strand and 11% β-turn. Like the β-strand and β-turn structures, the unordered structure also decreased with increasing TFE concentration.

CD spectra for pediocin AcH were also collected in SDS detergent (Figure 4). At the lowest concentration of SDS, 1 mM, one negative maximum at 222 nm and one positive maximum at 196 nm characterized the spectrum. The positive maximum was red shifted compared to the positive band typical of helix, indicating the presence of some β-structure (*32*). The CD spectra of pediocin AcH in higher SDS concentrations (5, 10, and 30 mM), above the CMC (4.5 mM) of SDS, showed characteristics of enhanced helical content. The tendency of submicellar concentrations of SDS to induce β-strand conformation, while α-helical structure is more likely to be induced by micellar concentrations, has

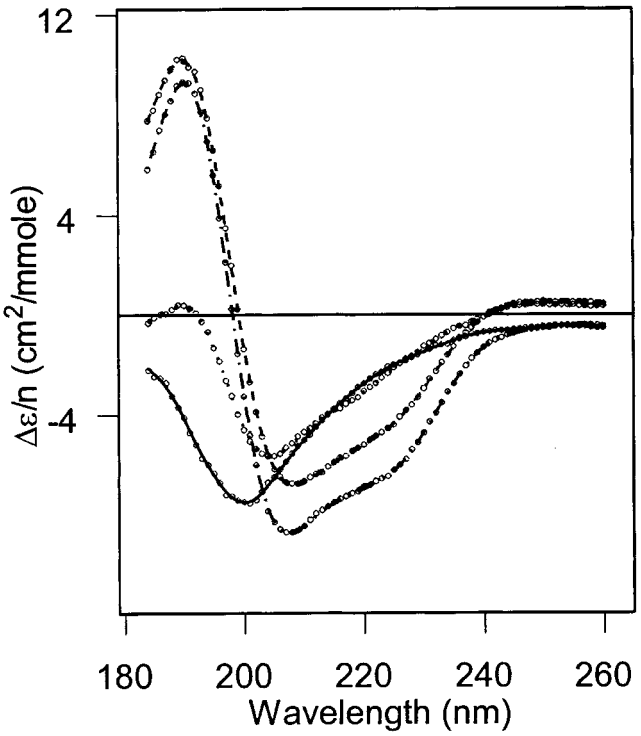

FIGURE 3: CD spectra of pediocin AcH in 10% TFE (—), 20% TFE (···), 50% TFE (---), and 90% TFE (—·—). Δϵ/n values are shown every nanometer (○). Curve fitting procedures are described under Experimental Procedures.

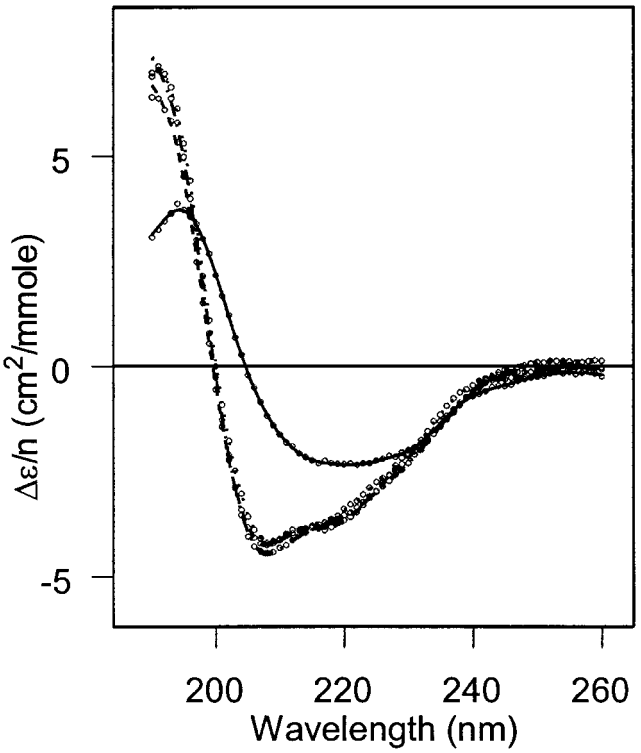

FIGURE 4: CD spectra of pediocin AcH in 1 mM SDS (—), 5 mM SDS (···), 10 mM SDS (—·—), and 30 mM SDS (---). Δϵ/n values are shown every nanometer (○). Curve fitting procedures are described under Experimental Procedures.

been reported previously (*31*). Quantitative analysis of the distribution of secondary structures (Table 2) showed substantial β-strand content (27%) induced in pediocin AcH

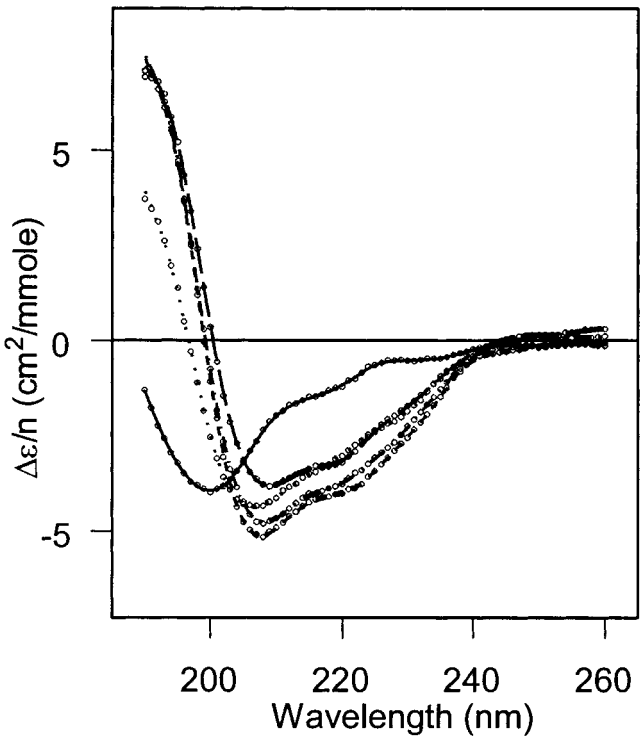

FIGURE 5: CD spectra of pediocin AcH in 0.5 mM DPC (—), 2 mM DPC (···), 5 mM DPC (—·—), 10 mM DPC (---), and 7 mM SDS−3 mM mixed micelles (— —). Δϵ/n values are shown every nanometer (○). Curve fitting procedures are described under Experimental Procedures.

by 1 mM SDS. The percentage of β-strand decreased substantially in micellar SDS concentrations to 15%−18%. Conversely, α-helical content increased to 36%−38% in micellar SDS concentrations, compared to 21% at submicellar concentrations. β-turn content was stable with increasing detergent concentration, as was the percentage of unordered structure.

To examine potential effects of detergent charge on structure, samples of pediocin AcH in the zwitterionic detergent, DPC, were examined (Figure 5). Spectra of peptide in 0.5 mM DPC, below the CMC for DPC (1.1 mM) (*52*), showed characteristics of unordered structure, but at micellar DPC concentrations, spectral features typical of α-helical structure became apparent. Quantitative analysis by CDPro (Table 2) verified that pediocin AcH was 63% unordered in 0.5 mM DPC. The percentage of unordered structure decreased in micellar DPC concentrations to 31%−35%. Likewise, the percentage of β-strand dropped consistently with increasing DPC concentration, and although the β-turn content initially increased with increasing DPC concentration, it gradually decreased above 2 mM DPC. Conversely, the α-helical content increased with increasing DPC until, in 10 mM DPC, pediocin AcH was 41% helical.

Although anionic lipid species predominate in peptide target organisms, no target contains 100% anionic phospholipids. Thus, scans were collected for peptide in 7 mM SDS−3 mM DPC mixed micelles (Figure 5). In these mixed micelles the peptide spectrum had features similar to those seen for pediocin AcH in micellar SDS concentrations. Quantitative analysis (Table 2) indicated that the peptide contained 34% α-helix, 20% β-strand, and 18% β-turn.

Comparison of the Spectra and Fractional Secondary Structures of Pediocin AcH in Vesicles versus TFE and Detergent Micelles. In comparing the distribution of secondary structures induced in pediocin AcH by various external environments, the accuracy of the curve fitting methods must be taken into account. The accuracy of SELCON, CDSSTR, and CONTIN/LL secondary structure estimation methods has been assessed (*40*). The performances of the analyses are characterized by RMS deviations (δ) and correlation coefficients (r) between X-ray and CD estimates of secondary structure fractions for each method. For the 48 protein reference set, taking into account all three estimation methods, the δ values for α-helix, β-sheet, β-turn ,and unordered secondary structure fractions are 0.08, 0.11, 0.07, and 0.08, respectively (N. Sreerama, personal communication). Therefore, only differences equal to or larger than these were considered significant when comparing the distribution of secondary structures induced in TFE and detergent micelles with the distribution in vesicles (Table 2). For α-helix, differences of less than 8% are really not significant; thus 20% TFE, 5−30 mM SDS, 2−5 mM DPC, and the SDS−DPC mixed micelles were considered satisfactory membrane mimetics for this particular secondary structure. The same screen, performed for β-strand, β-turn, and unordered secondary structures revealed that all solvents that induced the correct fraction of α-helical structure also induced correct fractions of all other secondary structures. Selected spectra for pediocin AcH, in the solvents identified as suitable by this screen, were qualitatively compared (Figure 6). The spectrum in 10 mM DPC was also included because the α-helix content differed by only 9% from that in vesicles, just beyond the allowed range. Only the spectrum of peptide in 20% TFE varied significantly from that seen for the peptide in vesicles and was eliminated as a satisfactory membrane mimetic. Thus, after both quantitative screening and qualitative curve comparisons, SDS, DPC, and the mixed detergent micelles were found to induce secondary structures comparable to those seen in vesicles. TFE−water mixtures and detergents below the CMC were not suitable mimics.

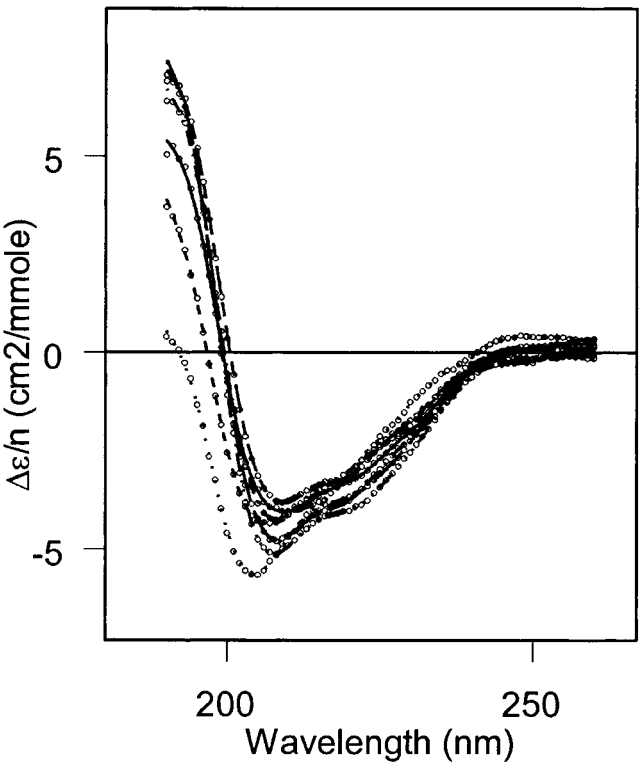

FIGURE 6: CD spectra of pediocin AcH in vesicles derived from *L. innocua* at a peptide to lipid molar ratio of 1/215 (—), 20% TFE (•••) 30 mM SDS (—•—), 2 mM DPC (---), 5 mM DPC (— —), 10 mM DPC (—•••—), and 7 mM SDS−3 mM DPC mixed micelles (— - —). $\Delta\epsilon/n$ values are shown every nanometer (○). Curve fitting procedures are described under Experimental Procedures. For simplicity of the figure, spectra for pediocin AcH in 5 mM SDS and 10 mM SDS were omitted. These curves were nearly identical in profile to that seen for peptide in 30 mM SDS (Figure 4).

DISCUSSION

It is proposed that, in the membrane-bound conformation of class IIa bacteriocins, the N-terminal amino acids fold into a three-strand β-sheet while a portion of the C-terminal residues forms an amphipathic α-helix (*20*, *21*, *25*, *27*). However, a peptide with a second disulfide bond, potentially able to affect the conformation of the C-terminal region, has never been structurally characterized. Therefore, the primary goals of this study were to examine and characterize the secondary structures of pediocin AcH in water and membrane vesicles. In addition, we wanted to identify environmental features necessary for structure induction.

CD analysis indicated that, like homologous peptides, pediocin AcH contains a great deal (>50%) of unordered sequence in aqueous buffer (*1*, *21*, *27*, *53*). An NMR study of leucocin A in 80% H_2O−10% D_2O−10% dimethyl sulfoxide (the latter added to improve solubility) showed no long-range NOEs characteristic of β-sheets and α-helices (*53*). CD spectra of leucocin A and carnobacteriocin B2 in water also have been described as reflecting an unordered conformation (*1*, *27*, *53*), but data were not presented. The CD spectrum of mesentericin $Y105^{37}$ in water has been reported (*21*), and because leucocin A differs from this peptide by only two residues, its spectrum may be similar. Interestingly, the mesentericin $Y105^{37}$ spectrum is very different from that of pediocin AcH, with a negative 200 nm band that is about 3-fold more intense and a less negative band in the 220 nm region. The spectrum is suggestive of a substantial amount of poly(Pro)II conformation (*54*), which is a left-handed 3-fold helix that is a significant component of many nominally unordered polypeptides. Interestingly, a mesentericin $Y105^{37}$ mutant lacking the disulfide bond actually gives a CD spectrum more similar to that of pediocin AcH in water.

The CD spectra of predominantly unordered peptides in water must be interpreted cautiously because the results of secondary structure calculations for such systems depend strongly on the reference proteins used (*47*). Nevertheless, our data indicate that some β-strand is present in pediocin AcH. This is made clear by comparing the fraction of β-strand in pediocin AcH with that observed in three denatured proteins at temperatures of 20 °C and below. Using the same reference set, output values for the denatured proteins are 8−12% β-strand (N. Sreerama, personal communication), compared with 20% β-strand for pediocin AcH. Taking the unfolded proteins as a rough baseline, the results suggest that the peptide contains at least 10% β-strand in water. This is consistent with the postulated N-terminal β-sheet occurring in a significant fraction of molecules. It is possible that the enhanced β-structure content may contribute

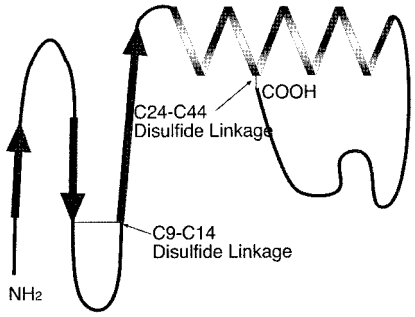

FIGURE 7: Proposed $\beta\alpha$ secondary structure of membrane-associated pediocin AcH. The β-structure, which accounts for 36% of the overall secondary structure, is speculated to be localized to the N-terminal region. 32% or 14 amino acids are helical and are predicted to localize to the C-terminal region (shown here between residues 19 and 32). Structural constraints imposed on the peptide by the presence of the helix would force the C-tail to loop back on the helix in order to form the C-terminal disulfide bond.

to the greater potency and activity spectrum seen for pediocin AcH. The folding of the β-structure in water may make available peptide surfaces needed for interactions with the membrane (*55*).

Upon binding to the membrane, pediocin AcH undergoes a substantial conformational reorganization: 32% or about 14 of the 44 amino acids were observed to be helical. This suggests that α-helical structure and perhaps the overall membrane permeabilizing structure are stabilized by membrane binding. On the basis of previous structural studies and predictions (*1, 25, 27*), it seems likely that the helical structure occurs within the C-terminal hydrophobic sequence region (W18−T35). As tryptophan residues commonly prefer to reside in electrostatically complex interfacial environments (*56*), perhaps the two tryptophan residues at positions 18 and 33 flank the helical segment. In this location, the helix would include C24, and its presence would create constraints forcing the C-tail to loop back onto the helix to form the C24−C44 disulfide bond. Although a chain length of 20 amino acids in α-helical conformation is required to span a bilayer, a 14-mer peptide has been shown to be capable of membrane perturbation (*57*).

In contrast to the striking increase observed in α-helical content, the percentages of β-strand and β-turn remained largely unchanged upon membrane binding. If the location of β-structure is the same, then it may be important not only to membrane binding but also to the final active conformation. The β-strand and β-turn structures in the membrane-bound peptide are predicted to localize to the N-terminal 17 residues (*28*). They constitute 36% or about 16 of the 44 peptide residues, making this β-region almost identical in size to that in leucocin A in 90% TFE and micellar DPC (*27*). Eight of the 16 β-residues are in β-turn conformation. Perhaps, 4 residues form the GNGV β-turn sequence and the other 4 create the rigid turn between the C9−C14 disulfide bond. A model depicting possible locations of structural elements is shown in Figure 7.

A number of systems considered to be membrane-like were investigated for their ability to induce a secondary structure distribution in pediocin AcH comparable to that induced by vesicles. Detergent micelles proved to be satisfactory membrane mimetics as they were able to induce secondary structure fractions comparable to those observed in vesicles. This demonstrates that the full complexity of a lipid bilayer with its two interfacial regions (*58*) is not essential for induction of the membrane-bound conformation. On the other hand, the inability of TFE to act as a membrane mimetic indicates the importance of the hydrocarbon−water interface to structure induction. We speculate that surface interactions are needed to maintain the correct proportions of β-sheet and α-helix secondary structures. The results also indicate that it is preferable to use micelles, rather than TFE, in NMR analysis of pediocin AcH structure.

In modeling the membrane-bound structure of pediocin AcH, interactions between peptide monomers that could alter structure must be considered. Pediocin AcH functions by forming pores in the membranes of target bacteria, which may require formation of assemblies containing several peptides (*7*). Thus, it is possible that the structures we have observed on membrane association are a consequence of peptide−peptide interactions. While quantification of pediocin AcH aggregation in the lipid bilayer is beyond the scope of this study, some information about this point can be obtained by considering the number of peptides actually present in vesicles and micelles. At the lowest peptide to phospholipid ratio (1/1125) there are 46−59 peptide molecules per vesicle assuming 1 phospholipid/60 Å^2 (T. Gutberlet, personal communication). At the highest peptide to phospholipid ratio (1/140) that induces an equivalent structure there are ~10-fold more peptides per vesicle. The fact that structure remains the same over this range suggests that peptide−peptide interactions are not playing a large role in structure induction. However, this 10-fold range may not be large enough to see the effects of cooperative structure induction if peptide aggregation occurs just as well at ca. 50 molecules per vesicle as at 500 molecules per vesicle. Thus, one should consider the number of peptides per micelle in systems that induce the same structure as formed in vesicles. At the lowest pediocin AcH to SDS molar ratio (assuming 33 SDS molecules per micelle) (*59*), there are 0.02 peptide per micelle. At this ratio, it seems unlikely that structure is influenced by peptide−peptide interactions. We conclude that structure changes observed in the peptide in the presence of vesicles are caused primarily by membrane binding.

A comparison of the structures of pediocin AcH, leucocin A, and carnobacteriocin B2 in 90% TFE shows that the folding of these peptides differs widely in this solvent. In leucocin A, 90% TFE induces an N-terminal three-strand antiparallel β-sheet and a C-terminal amphipathic α-helix (*27*). This differs substantially from the single, longer helix induced in carnobacteriocin B2 with no accompanying β-structure (*1*). Pediocin AcH takes on a greater percentage helicity (66%) in 90% TFE than the other two peptides and, due to conformational constraints imposed on the central region by disulfide bonds, may contain two helical segments. The β-structure induced by 90% TFE in pediocin AcH is smaller than that in leucocin A and greater than that seen in carnobacteriocin B2 (*1*, *27*). On first observing these differences, it is tempting to make inferences about why target specificity and bactericidal spectrum vary for these peptides. However, the current study has stressed the importance of environment to appropriate structure induction. It seems very possible that the variation in structure could ultimately be due only to the differing effects of TFE on the bacteriocins.

As noted by Wang et al. (*1*), TFE is known to stabilize amphipathic structures (*60*, *61*). Thus, the varying amphipathic nature of the peptides' main sequence elements could strongly influence the structures induced by this solvent.

In summary, unlike related bacteriocins, pediocin AcH contains some β-structure in aqueous solution. In membrane vesicles the peptide undergoes conformational changes to take on a mixed $\beta\alpha$ secondary structure. The superiority of detergent micelles over TFE in appropriately mimicking the membrane environment demonstrates that a hydrocarbon−water interface is important for proper induction of the active conformation of pediocin AcH.

ACKNOWLEDGMENT

The authors thank Doug E. Kamen, Conrad E. Schaefer, and A-Young Moon Woody for advice and technical assistance with CD experiments. A warm thanks is also extended to Narasimha Sreerama for continuous advice and recommendations for the use of the CDPro software analysis program. Peptide isolation and purification were made possible thanks to the work of Robin Schamber.

REFERENCES

1. Wang, Y., Henz, M. E., Fregeau Gallagher, N. L., Chai, S., Gibbs, A. C., Yan, L. Z., Stiles, M. E., Wishart, D. S., and Vederas, J. C. (1999) *Biochemistry 38*, 15438−15447.
2. Ge, Y., MacDonald, D. L., Holroyd, K. J., Thornsberry, C., Wexler, H., and Zasloff, M. (1999) *Antimicrob. Agents Chemother. 43*, 782−788.
3. Severina, E., Severina, A., and Tomasz, A. (1998) *J. Antimicrob. Chemother. 41*, 341−347.
4. Ray, B., and Miller, K. W. (2000) in *Natural food antimicrobial systems* (Naidu, A. S., Ed.) pp 525−566, CRC Press, Washington, DC.
5. Jack, R. W., Tagg, J. R., and Ray, B. (1995) *Microbiol. Rev. 59*, 171−200.
6. Chikindas, M. L., Garcia-Garcera, M. J., Driessen, A. J., Ledeboer, A. M., Nissen-Meyer, J., Nes, I. F., Abee, T., Konings, W. N., and Venema, G. (1993) *Appl. Environ. Microbiol. 59*, 3577−3584.
7. Ennahar, S., Shaihara, T., Sonomoto, K., and Ishizaki, A. (2000) *FEMS Microbiol. Rev. 24*, 85−106.
8. Bhugaloo-Vial, P., Douliez, J. P., Molle, D., Dousset, X., Boyaval, P., and Marion, D. (1999) *Appl. Environ. Microbiol. 65*, 2895−2900.
9. Hastings, J. W., Sailer, M., Johnson, K., Ray, K. W., Vederas, J. C., and Stiles, M. E. (1991) *J. Bacteriol. 173*, 7491−7500.
10. Hechard, Y., Derijard, B., Letellier, F., and Concenatiempo, Y. (1992) *J. Gen. Microbiol. 138*, 2725−2731.
11. Henderson, J. T., Chopko, A. L., and VanWassenaar, P. D. (1992) *Arch. Biochem. Biophys. 295*, 5−12.
12. Holck, A., Axelsson, L., Birkeland, E., Aukrust, T., and Bloom, H. (1992) *J. Gen. Microbiol. 138*, 2715−2720.
13. Holck, A., Axelsson, L., Huhne, K., and Krockel, L. (1994) *FEMS Microbiol. Rev. 115*, 143−150.
14. Le Marrec, C., Hyronimus, B., Bressollier, P., Verneuil, B., and Urdaci, M. C. (2000) *Appl. Environ. Microbiol. 66*, 5213−5220.
15. Marugg, J. D., Gonzalez, C. F., Kunka, B. S., Ledeboer, A. M., Pucci, M. J., Toonen, M. Y., Walker, S. A., Zoetmulder, L. C., and Vandenbergh, P. A. (1992) *Appl. Environ. Microbiol. 58*, 2360−2367.
16. Motlagh, A. M., Bhunia, A. K., Szostec, F., Hanson, T. R., Johnson, M. C., and Ray, B. (1992) *Lett. Appl. Microbiol. 15*, 45−48.
17. Quadri, L. E. N., Sailer, M., Roy, K. L., Vederas, J. C., and Stiles, M. E. (1994) *J. Biol. Chem. 269*, 12204−12211.
18. Tickhaczek, P. S., Vogel, R. S., and Hammes, W. P. (1993) *Arch. Microbiol. 160*, 279−283.
19. Eijsink, V. G. H., Skeie, H., Middelhoven, P. H., Brurberg, M. B., and Nes, I. F. (1998) *Appl. Environ. Microbiol. 64*, 3275−3281.
20. Fimland, G., Blingsmo, O. R., Sletten, K., Jung, G., Nes, I. F., and Nissen-Meyer, J. (1996) *Appl. Environ. Microbiol. 62*, 3313−3318.
21. Fleury, Y., Dayem, J. J., Montagne, E., Chaboisseau, J. P., Le Caer, P., Nicolas, P., and Deflour, A. (1996) *J. Biol. Chem. 271*, 14421−14429.
22. Ray, B., Schamber, R., and Miller, K. W. (1999) *Appl. Environ. Microbiol. 65*, 2281−2286.
23. Miller, K. W., Schamber, R., Osmanagaoglu, O., and Ray. B. (1998) *Appl. Environ. Microbiol. 64*, 1997−2005.
24. Fimland, G., Johnson, L., Axelsson, L., Brurberg, M. B., Nes, I. F., Eijsink, V. G. H., and Nissen-Meyer, J. (2000) *J. Bacteriol. 182*, 2643−2648.
25. Bhugaloo-Vial, P., Dousset, X., Metivier, O., Sorokine, P., Anglade, P., Boyaval, P., and Marion, D. (1996) *Appl. Environ. Microbiol. 62*, 4410−4416.
26. Cintas, I., Casaus, P., Halvarstein, L. S., Hernandez, P. E., and Nes, I. F. (1997) *Appl. Environ. Microbiol. 63*, 4321−4330.
27. Fregeau Gallagher, N. L., Sailer, M., Niemczura, W. P., Nakashima, T. T., Stiles, M. E., and Vederas, J. C. (1997) *Biochemistry 36*, 15062−15072.
28. Chen, Y., Shapira, R., Eisenstein, M., and Montville, T. J. (1997) *Appl. Environ. Microbiol. 63*, 524−531.
29. Baleja, J. D. (2001) *Anal. Biochem. 288*, 1−15.
30. Wallace, B. A., Veatch, W. R., and Blout, E. R. (1981) *Biochemistry 20*, 5754−5760.
31. Zhong, L., and Johnson, W. C. (1992) *Proc. Natl. Acad. Sci. U.S.A. 89*, 4462−4465.
32. Woody, R. W. (2001) in *Synthesis of peptides and peptidomimetics* (Goodman, M., Felix, A., Moroder, L., and Toniolo, C., Eds.) Vol. E22a, Houben-Weyl Methods of Organic Chemistry, Georg Thieme Verlag, Stuttgart (in press).
33. Ray, S. K., Kim, W. J., Johnson, M. C., and Ray, B. (1992) *J. Appl. Bacteriol. 66*, 393−399.
34. Yang, R., Johnson, M. C., and Ray, B. (1992) *Appl. Environ. Microbiol. 58*, 3355−3359.
35. Kates, M. (1986) in *Techniques in biochemistry and molecular biology* (Burdon, R. H., and van Knippenberg, P. H., Eds.) pp 100−108, Elsevier, Amsterdam.
36. New, R. R. C. (1992) in *Liposomes: a practical approach*, pp 105−109, 256−257, IRL Press, Oxford.
37. Winkowski, K., Ludescher, R. D., and Montville, T. J. (1995) *Appl. Environ. Microbiol. 62*, 323−327.
38. Vulliez-Le Normand, B., and Eisele, J.-L. (1993) *Anal. Biochem. 208*, 241−243.
39. Heyn, M. P. (1989) *Methods Enzymol. 172*, 575−584.
40. Sreerama, N., and Woody, R. W. (2000) *Anal. Biochem. 287*, 252−260.
41. Provencher, S. W. (1982) *Comput. Phys. Commun. 27*, 213−227.
42. Sreerama, N., and Woody, R. W. (1993) *Anal. Biochem. 209*, 32−44.
43. Forsythe, G. E., Malcolm, M. A., and Moler, C. B. (1977) *Computer Methods for Mathematical Computations*, Prentice Hall, Upper Saddle River, NJ.
44. Manavalan, P., and Johnson, W. C., Jr. (1987) *Anal. Biochem. 167*, 76−85.
45. van Stokkum, I. H. M., Spoelder, H. J. W., Bloemendal, M., van Grondelle, R., and Groen, F. C. A. (1990) *Anal. Biochem. 191*, 110−118.
46. Johnson, W. C., Jr. (1999) *Proteins: Struct., Funct., Genet. 35*, 307−312.
47. Sreerama, N., Venyaminov, S. Y., and Woody, R. W. (2000) *Anal. Biochem. 287*, 243−251.
48. Fasman, G. D. (1996) in *Circular Dichroism and the Conformational Analysis of Biomolecules* (Fasman, G. D., Ed.) pp 381−412, Plenum Press, New York.

49. Li, S.-C., and Deber, C. M. (1994) *Nat. Struct. Biol. 1*, 368−373.
50. Gans, P. J., Lyu, P. C., Manning, M. C., Woody, R. W., and Kallenbach, N. R. (1991) *Biopolymers 31*, 6105−6114.
51. Blundell, T., Barlow, D., Borkakoti, N., and Thornton, J. (1983) *Nature 306*, 281−283.
52. Lauterwein, J., Bosch, C., Brown, L. R., and Wuthrich, K. (1979) *Biochim. Biophys. Acta 556*, 244−246.
53. Sailer, M., Helms, G. L., Henkel, T., Niemczura, W. P., Stiles, M. E., and Vederas, J. C. (1993) *Biochemistry 32*, 310−318.
54. Woody, R. W. (1992) *Adv. Biophys. Chem. 2*, 37−79.
55. Segrest, J. P., De Loof, H., Dohlman, J. G., Brouillette, C. G., and Anantharamaiah, G. M. (1990) *Proteins: Struct., Funct., Genet. 8*, 103−117.
56. Yau, W., Wimley, W. C., Gawrisch, K., and White, S. H. (1998) *Biochemistry 37*, 14713−14718.
57. Park, N. G., Yamato, Y., Lee, S., and Sugihara, G. (1995) *Biopolymers 36*, 793−801.
58. White, S. H., and Wimley, W. C. (1998) *Biochim. Biophys. Acta 1376*, 339−352.
59. Shaw, D. J. (1970) *Introduction to Colloid and Surface Chemistry*, Butterworths, Boston.
60. Merutka, G., and Stellwagen, E. (1989) *Biochemistry 28*, 352−357.
61. Nelson, J. W., and Kallenbach, N. R. (1989) *Biochemistry 28*, 5256−5261.

BI011031P